Available online at www.sciencedirect.com

SciVerse ScienceDirect

Journal of the European Ceramic Society 32 (2012) 1485–1489

www.elsevier.com/locate/jeurceramsoc

Short Communication

Synthesis, electromagnetic reflection loss and oxidation resistance of pyrolytic carbon-Si_3N_4 ceramics with dense Si_3N_4 coating

Xiangming Li [a,*], Litong Zhang [b], Xiaowei Yin [b]

[a] College of Water Resources and Architecture Engineering, Northwest Agriculture and Forestry University, Yangling, Shaanxi 712100, PR China
[b] National Key Laboratory of Thermostructure Composite Materials, Northwestern Polytechnical University, Xi'an, Shaanxi 710072, PR China

Received 17 October 2011; received in revised form 20 January 2012; accepted 25 January 2012
Available online 16 February 2012

Abstract

Si_3N_4-coated porous pyrolytic carbon-Si_3N_4 ceramics (PyC-Si_3N_4/Si_3N_4) were fabricated by chemical vapour infiltration of PyC into porous Si_3N_4 ceramic and then chemical vapour deposition of Si_3N_4 coating on the surface of the obtained PyC-Si_3N_4. The PyC-Si_3N_4/Si_3N_4 with 3.1 vol.% PyC content possesses electromagnetic reflection loss as low as −11.5 dB. Due to the excellent sealing effect of dense Si_3N_4 coating, the PyC-Si_3N_4/Si_3N_4 possesses good oxidation resistance, which makes PyC-Si_3N_4/Si_3N_4 a good electromagnetic absorbing material that can be used at temperature as high as 1100 °C.

Keywords: Si_3N_4; Porosity; Carbon; Chemical vapour deposition; Functional applications

1. Introduction

Reflection and absorption are two different ways in attenuating electromagnetic radiation. A common way of shielding electromagnetic wave is using materials with high conductivity, such as metal, as a shielding package. With the development of radar and microwave communication technology, it is in dire need of anti-electromagnetic interference technology, self-concealing materials and microwave darkrooms. It is known that the shielding of electromagnetic wave by absorption is more useful than that by reflection.

Compared with metal, carbon possesses good electromagnetic attenuating property and environmental stability, so carbon is a good absorbing agent which is usually added into another matrix to improve electromagnetic absorbing property. The electromagnetic shielding properties of polymers and ceramics containing carbon-based fillers (e.g., carbon blacks,[1,2] graphite flakes,[3] carbon fibres[4,5] and nanotubes [6–10]) have been extensively investigated. Due to the high electrical conductivity of carbon, above materials shield electromagnetic wave mainly by reflection.[11,12] In addition, because of the bad oxidation resistance of carbon, these materials can only be used at temperatures below 500 °C. Therefore, it is in dire need of fabricating carbon-based material not only with low electromagnetic reflection loss, but also with good oxidation resistance.

As known from our previous work,[13] porous Si_3N_4 ceramic with dense Si_3N_4 coating (Si_3N_4/Si_3N_4) possesses good moisture resistance because of the sealing effect of dense Si_3N_4 coating. In the present work, pyrolytic carbon-Si_3N_4 ceramics (PyC-Si_3N_4) are fabricated by chemical vapour infiltration (CVI) of PyC into porous Si_3N_4 ceramic, and then PyC-Si_3N_4 ceramics with dense Si_3N_4 coating (PyC-Si_3N_4/Si_3N_4) are fabricated by chemical vapour deposition (CVD) of Si_3N_4 coating on the surface of the obtained PyC-Si_3N_4. The effect of PyC content on the electromagnetic reflection loss of PyC-Si_3N_4/Si_3N_4 and the effect of dense Si_3N_4 coating on the oxidation resistance of PyC-Si_3N_4/Si_3N_4 are investigated in detail.

2. Experimental

2.1. Sample preparation

Porous Si_3N_4 ceramic fabricated in our previous work was machined into samples with dimensions of 2.8 mm × 10.1 mm × 22.8 mm. PyC was infiltrated into the samples by CVI using butane as precursor at 870 °C and a

* Corresponding author. Tel.: +86 29 87082902; fax: +86 29 87082901.
E-mail address: li_xiangming@yahoo.com (X. Li).

0955-2219/$ – see front matter © 2012 Elsevier Ltd. All rights reserved.
doi:10.1016/j.jeurceramsoc.2012.01.027

reduced pressure of 500 Pa. Si_3N_4 coating was deposited on the surface of the samples by CVD using silicon tetrachloride ($SiCl_4 \geq 99.99$ wt.%) and ammonia gas ($NH_3 \geq 99.99\%$) as precursors at 1100 °C and a reduced pressure of 2 kPa in argon atmosphere.[13]

2.2. Characterization

The porosity was measured by Archimedes method. The microstructure was observed by scanning electron microscopy (SEM, S-4700, Hitachi, Japan). The electromagnetic absorbing property was determined by calculating the electromagnetic reflection loss according to Eq. (1) shown as follows:

$$R = 20 \log \left| \frac{Z_{in} - 1}{Z_{in} + 1} \right| \quad (1)$$

where Z_{in} is the normalized input impedance of the electromagnetic absorption layer which is calculated according to Eq. (2) shown as follows:

$$Z_{in} = \sqrt{\frac{\mu_r}{\varepsilon_r}} \tanh \left(j \frac{2\pi}{c} \sqrt{\mu_r \varepsilon_r} fd \right) \quad (2)$$

where c is the light velocity in vacuum, f is the electromagnetic wave frequency, d is the thickness of the absorber, ε_r and μ_r are the relative permittivity and permeability of the absorber, respectively. In the present work, μ_r was taken as 1.0 because of the negligible magnetic property of PyC-Si_3N_4/Si_3N_4 ceramics. ε_r in frequency of 8.2–12.4 GHz is measured by vector network analyzer (VNA, MS4644A, Anritsu, Japan).

Table 1
Open porosities of PyC-Si_3N_4 and PyC-Si_3N_4/Si_3N_4 with different PyC content.

PyC-Si_3N_4		PyC-Si_3N_4/Si_3N_4	
PyC content (vol.%)	Open porosity (%)	PyC content (vol.%)	Open porosity (%)
0	46	0	0
1.1	45	1.0	0
2.0	44	1.9	0
3.2	42	3.1	0
5.6	40	5.4	0
7.7	38	7.5	0

3. Results and discussion

3.1. Microstructure and porosity

Fig. 1 shows the micrographs of Si_3N_4/Si_3N_4 and PyC-Si_3N_4/Si_3N_4. As can be seen, the PyC is uniformly distributed in porous Si_3N_4. The dense Si_3N_4 coating is about 30 μm thick and crack free. Table 1 lists the open porosities of PyC-Si_3N_4 and PyC-Si_3N_4/Si_3N_4 with different PyC content. By increasing CVI time, the PyC-Si_3N_4 with PyC content of 1.1, 2.0, 3.2, 5.6 and 7.7 vol.% are fabricated, respectively. Actually, the total amount of PyC in PyC-Si_3N_4 remains unchanged after CVD of Si_3N_4, but the content of PyC in PyC-Si_3N_4/Si_3N_4 decreases slightly because of the increase of sample bulk. Here, the content of PyC in PyC-Si_3N_4/Si_3N_4 is 1.0, 1.9, 3.1, 5.4 and 7.5 vol.%, respectively. Amazingly, no matter what content of PyC in PyC-Si_3N_4/Si_3N_4 is, the open porosity of PyC-Si_3N_4/Si_3N_4 is 0% due to the excellent sealing effect of dense Si_3N_4 coating.

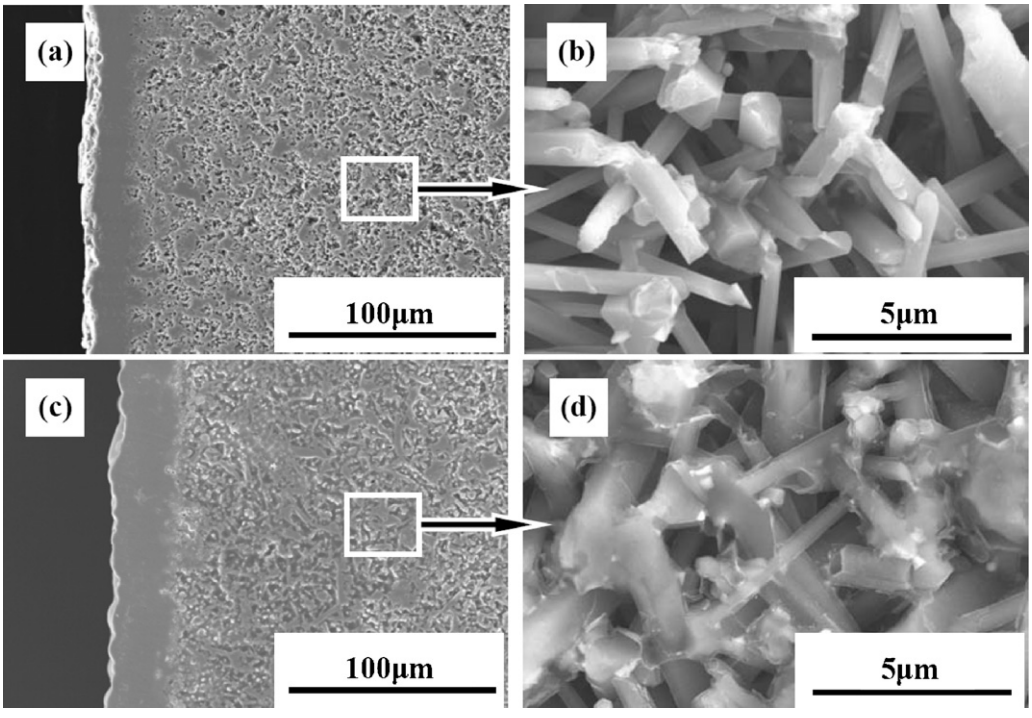

Fig. 1. Micrographs of (a, b) Si_3N_4/Si_3N_4 and (c, d) PyC-Si_3N_4/Si_3N_4.

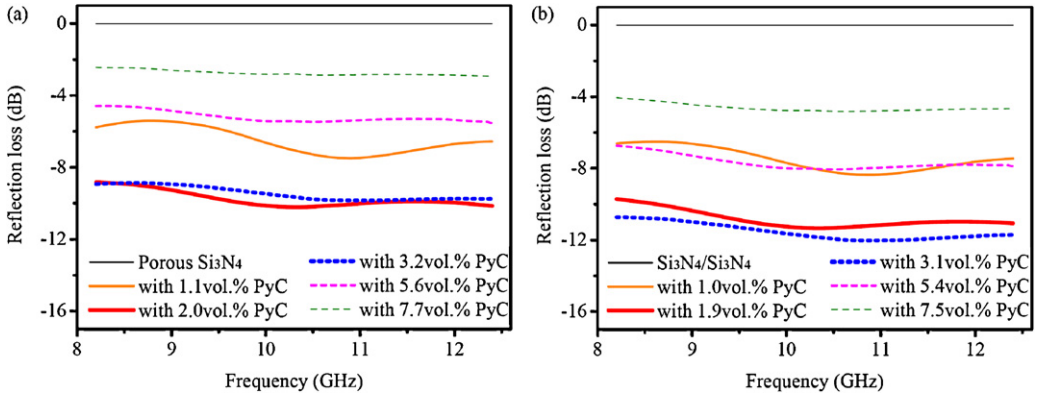

Fig. 2. Reflection losses of (a) PyC-Si_3N_4 and (b) PyC-Si_3N_4/Si_3N_4 with different PyC content.

3.2. Reflection loss of PyC-Si_3N_4 and PyC-Si_3N_4/Si_3N_4

The electromagnetic reflection loss of a material is codetermined by the reflection of electromagnetic wave occurring on the surface of the material and by the absorption of electromagnetic wave in the material. As shown in Fig. 2(a), due to the improvement of electromagnetic wave absorption ability, the mean reflection loss of PyC-Si_3N_4 decreases from −6.5 to −9.8 dB with the increase of PyC content from 1.1 to 2.0 vol.%. The electromagnetic wave absorption ability of PyC-Si_3N_4 is further improved with the increase of PyC content from 2.0 to 7.7 vol.%, but the electromagnetic wave is reflected more on the surface of PyC-Si_3N_4 because of the aggravation of impedance break between air and PyC-Si_3N_4. When the electromagnetic wave enters PyC-Si_3N_4, the absorption of electromagnetic wave can occur, so the mean reflection loss of PyC-Si_3N_4 increases from −9.8 to −2.7 dB with the increase of PyC content from 2.0 to 7.7 vol.%.

After CVD of Si_3N_4, the amount of electromagnetic wave reflected on the surface of PyC-Si_3N_4/Si_3N_4 decreases obviously because the impedance break between air and PyC-Si_3N_4 is weakened by Si_3N_4 coating. The dense Si_3N_4 coating improves the entry of electromagnetic waves into PyC-Si_3N_4/Si_3N_4, where they can be absorbed. The comparison of reflection losses of the samples with the same PyC content, but without or with CVD Si_3N_4 coating shows [Fig. 2(a) and (b)] that PyC-Si_3N_4/Si_3N_4 possesses lower reflection loss than PyC-Si_3N_4. The mean reflection loss of PyC-Si_3N_4/Si_3N_4 with 3.1 vol.% PyC content reaches −11.5 dB [Fig. 2(b)], while it is −9.5 dB for PyC-Si_3N_4 with 3.2 vol.% PyC content [Fig. 2(a)].

3.3. Oxidation resistance of PyC-Si_3N_4 and PyC-Si_3N_4/Si_3N_4

The majority of carbon-based materials, including PyC-Si_3N_4 possess bad oxidation resistance. Fig. 3(a) shows the weight change of PyC-Si_3N_4 sample with 2.0 vol.% PyC content after oxidation at 700 °C. The weight of PyC-Si_3N_4 sample decreases gradually as the oxidation time increases from 1 to 5 h due to the oxidation of PyC in PyC-Si_3N_4. As the oxidation time increases to more than 5 h the PyC is completely burned out in PyC-Si_3N_4 sample, so the weight of PyC-Si_3N_4 sample remains unchanged with the time of oxidation.

Fig. 3(b) shows the weight change of PyC-Si_3N_4/Si_3N_4 samples with PyC content of 1.0, 3.1 and 7.5 vol.% respectively after oxidation at 700–1300 °C for 10 h. As can be seen, the weight of PyC-Si_3N_4/Si_3N_4 samples increases slightly with the increase of oxidation temperature from 700 to 1100 °C, and then decreases rapidly when the oxidation temperature reaches 1300 °C. The oxidation product of Si_3N_4 is amorphous silica when Si_3N_4 is oxidized at temperatures below 1100 °C.[14] The little increase of PyC-Si_3N_4/Si_3N_4 samples in weight after oxidation at 900 °C and 1100 °C is due to the oxidation of Si_3N_4 coating. When the oxidation temperature reaches 1300 °C, the oxidation rate of Si_3N_4 coating increases and the oxidation-derived silica transforms into cristobalite quickly.[15] Because there is a significant difference in the coefficient of thermal expansion (CTE) between silica and cristobalite, the transformation from silica to cristobalite initiates crack formation in the dense Si_3N_4 coating. Afterwards oxygen can penetrate through the cracked Si_3N_4 coating and react with PyC in the porous PyC-Si_3N_4 body. Therefore, the rapid weight decrease of the PyC-Si_3N_4/Si_3N_4 samples after oxidation at 1300 °C for 10 h is due to the oxidation of PyC.

The oxidation test of PyC-Si_3N_4/Si_3N_4 sample with 3.1 vol.% PyC at 1300 °C shows a small weight change up to 4 h [Fig. 3(c)]. During the oxidation process PyC and Si_3N_4 are oxidized at the same time. The oxidation of PyC decreases the weight of sample due to the formation of CO and CO_2 gases, while the oxidation of Si_3N_4 is connected by weight gain. At the beginning of oxidation process, oxygen can hardly enter the Si_3N_4-coated PyC-Si_3N_4/Si_3N_4 sample because there are only few small cracks in Si_3N_4 coating, so the amount of PyC in PyC-Si_3N_4/Si_3N_4 remains almost unchanged. The weight of PyC-Si_3N_4/Si_3N_4 sample increases at the beginning of oxidation process, because the oxidation rate of Si_3N_4 coating is faster than that of PyC under this protecting layer. As the oxidation time increases from 2 to 10 h, the number and size of cracks in Si_3N_4 coating increases, it is easier for oxygen to enter the porous PyC-Si_3N_4 body and react with PyC. The weight of PyC-Si_3N_4/Si_3N_4 sample decreases rapidly because the oxidation rate of PyC is faster than that of Si_3N_4. As the oxidation time increases to more than 10 h, the PyC is completely burned out in PyC-Si_3N_4/Si_3N_4

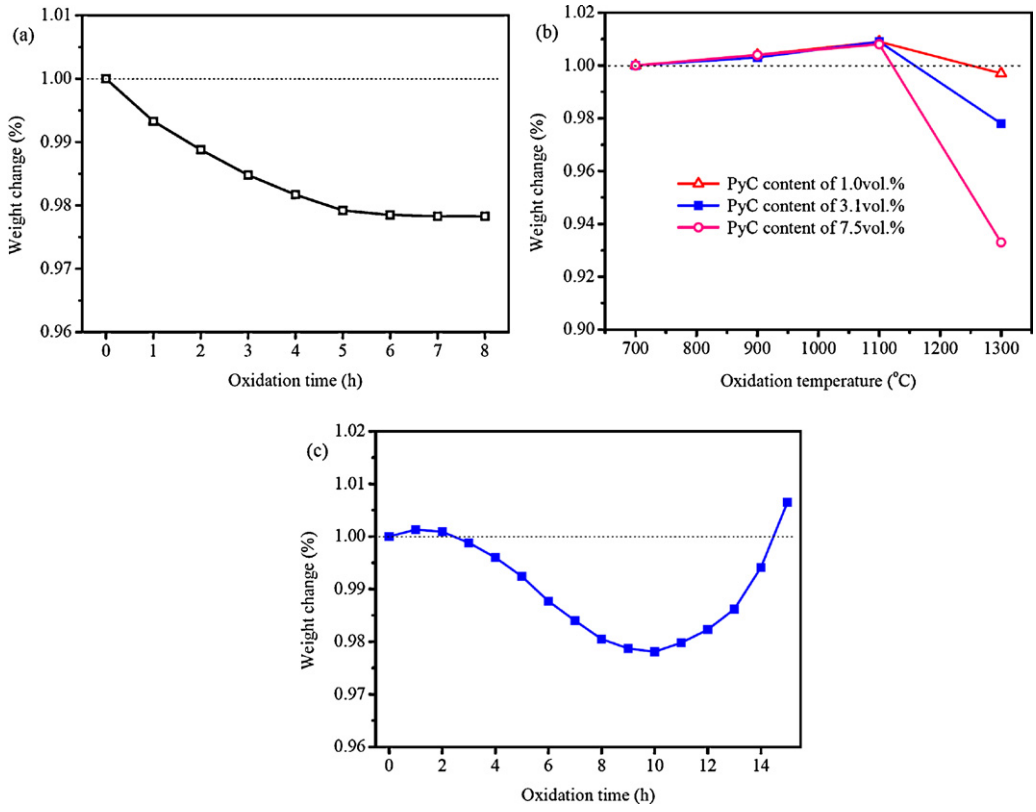

Fig. 3. Weight changes of (a) PyC-Si_3N_4 sample with 2.0 vol.% PyC content after oxidation at 700 °C, (b) PyC-Si_3N_4/Si_3N_4 samples with PyC content of 1.0, 3.1 and 7.5 vol.% respectively after oxidation at 700–1300 °C for 10 h, and (c) PyC-Si_3N_4/Si_3N_4 sample with 3.1 vol.% PyC content after oxidation at 1300 °C.

sample. However, the oxidation of Si_3N_4 further proceeds, so the weight of PyC-Si_3N_4/Si_3N_4 sample again increases with the time of oxidation.

3.4. Reflection loss of PyC-Si_3N_4 and PyC-Si_3N_4/Si_3N_4 after oxidation

Fig. 4 shows the reflection losses of PyC-Si_3N_4 with 2.0 vol.% PyC content after oxidation at 700 °C, and that of PyC-Si_3N_4/Si_3N_4 with 3.1 vol.% PyC content after oxidation at 1100 °C. The mean reflection loss of PyC-Si_3N_4 increases obviously from −7.0 to −0.3 dB with the increase of oxidation time from 1 to 5 h at 700 °C [Fig. 4(a)], because the content of PyC in PyC-Si_3N_4 decreases. Contrary, in PyC-Si_3N_4/Si_3N_4 sample the PyC is not oxidized at 1100 °C due to the protection of Si_3N_4 coating, but there is a thin SiO_2 layer formed at the surface of Si_3N_4 coating. Theoretically, SiO_2 layer has little effect on the reflection loss of PyC-Si_3N_4/Si_3N_4 because SiO_2 is a good wave-transparent material. However, SiO_2 layer can weaken the impedance break between air and Si_3N_4 coating, which makes easier the entry of electromagnetic waves into PyC-Si_3N_4/Si_3N_4 sample. Therefore, the mean reflection loss of PyC-Si_3N_4/Si_3N_4 after 2 h oxidation is −11.8 dB, which is only a little lower than that for as-obtained PyC-Si_3N_4/Si_3N_4 [Fig. 4(b)]. Once SiO_2 layer forms, the little increase of the thickness of SiO_2 layer has no effect on the impedance break between air and Si_3N_4 coating,

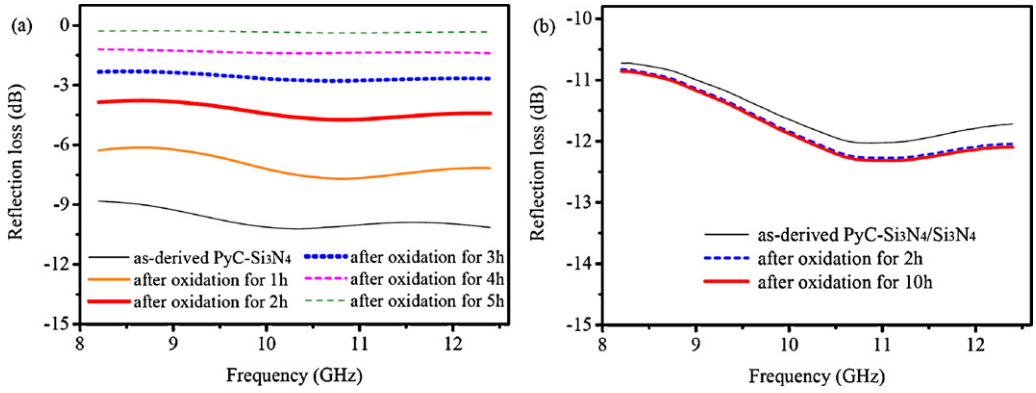

Fig. 4. Reflection losses of (a) PyC-Si_3N_4 with 2.0 vol.% PyC content after oxidation at 700 °C, and (b) PyC-Si_3N_4/Si_3N_4 with 3.1 vol.% PyC content after oxidation at 1100 °C.

so the reflection loss of PyC-Si_3N_4/Si_3N_4 remains unchanged as the oxidation time increases from 2 to 10 h.

4. Conclusions

In this study the fabrication of Si_3N_4-coated porous PyC-Si_3N_4/Si_3N_4 ceramic was done by CVI of PyC into porous Si_3N_4 ceramic and by subsequent CVD of Si_3N_4 coating on its surface. The electromagnetic reflection loss of PyC-Si_3N_4/Si_3N_4 with 3.1 vol.% PyC content reaches −11.5 dB. Because of the excellent sealing effect of dense Si_3N_4 coating, the PyC-Si_3N_4/Si_3N_4 possesses remarkable oxidation resistance. The PyC-Si_3N_4/Si_3N_4 is a good electromagnetic absorbing material not only at room temperature but also at temperatures as high as 1100 °C.

References

1. Im JS, Kim JG, Lee YS. Fluorination effects of carbon black additives for electrical properties and EMI shielding efficiency by improved dispersion and adhesion. *Carbon* 2009;**47**(11):2640–7.
2. Kwon SK, Ahn JM, Kim GH, Chun CH, Hwang JS, Lee JH. Microwave absorbing properties of carbon black/silicone rubber blend. *Polym Eng Sci* 2002;**42**(11):2165–71.
3. Luo XC, Chung DDL. Electromagnetic interference shielding reaching 130 dB using flexible graphite. *Carbon* 1996;**34**(10):1293–4.
4. Cao MS, Song WL, Hou ZL, Wen B, Yuan J. The effects of temperature and frequency on the dielectric properties, electromagnetic interference shielding and microwave-absorption of short carbon fiber/silica composites. *Carbon* 2010;**48**(3):788–96.
5. Huang CY, Mo WW, Roan ML. Studies on the influence of double-layer electroless metal deposition on the electromagnetic interference shielding effectiveness of carbon fiber/ABS composites. *Surf Coat Technol* 2004;**184**(2–3):163–9.
6. Fugetsu B, Sano E, Sunada M, Sambongi Y, Shibuya T, Wang XS, et al. Electrical conductivity and electromagnetic interference shielding efficiency of carbon nanotube/cellulose composite paper. *Carbon* 2008;**46**(9):1256–8.
7. Al-Saleh MH, Sundararaj U. Electromagnetic interference shielding mechanisms of CNT/polymer composites. *Carbon* 2009;**47**(7):1738–46.
8. Song WL, Cao MS, Hou ZL, Yuan J, Fang XY. High-temperature microwave absorption and evolutionary behavior of multiwalled carbon nanotube nanocomposite. *Scripta Mater* 2009;**61**(2):201–4.
9. Shi SL, Liang J. The effect of multi-wall carbon nanotubes on electromagnetic interference shielding of ceramic composites. *Nanotechnology* 2008;**19**(25):255707-1–5.
10. Shi SL, Liang J. Electronic transport properties of multiwall carbon nanotubes/yttria-stabilized zirconia composites. *J Appl Phys* 2007;**101**(2):023708-1–5.
11. Chen B, Wu K, Yao W. Conductivity of carbon fiber reinforced cement-based composites. *Cement Concrete Compos* 2004;**26**(4):291–7.
12. Chung DDL. Electrical conduction behavior of cement–matrix composites. *J Mater Eng Perform* 2002;**11**(2):194–204.
13. Li XM, Yin XW, Zhang LT, Pan TH. Comparison in microstructure and mechanical properties of porous Si_3N_4 ceramics with SiC and Si_3N_4 coatings. *Mater Sci Eng A* 2009;**527**(1–2):103–9.
14. Li XM, Yin XW, Zhang LT, Cheng LF, Qi YC. Mechanical and dielectric properties of porous Si_3N_4–SiO_2 composite ceramics. *Mater Sci Eng A* 2009;**500**(1–2):63–9.
15. Li XM, Yin XW, Zhang LT, He SS. The devitrification kinetics of silica powder heat-treated in different conditions. *J Non-Cryst Solids* 2008;**354**(28):3254–9.